



# Recycled sand for sustainable 3D-printed sand mold processes

Yen-Ting Li<sup>1</sup> · Yih-Lin Cheng<sup>1</sup> · Kea-Tiong Tang<sup>2</sup>

Received: 14 May 2023 / Accepted: 23 August 2023 / Published online: 25 August 2023  
© The Author(s), under exclusive licence to Springer-Verlag London Ltd., part of Springer Nature 2023

## Abstract

Traditional casting methods are losing their appeal due to poor working conditions. Integrating additive manufacturing into traditional Casting is a popular solution. Among the seven additive manufacturing categories, binder jet 3D printing is most suitable for 3D printing sand molds. However, issues like waste management and environmental problems in binder jetting need to be solved. The investigation proves that utilizing recycled sand as a raw material for 3D printing sand products can reduce the environmental impacts associated with binder jet 3D printing while achieving adequate mechanical properties. This study shows that recycled sand can produce mechanical properties comparable to new sand, while reducing waste and environmental impact. The study examines samples of new sand and recycled sand obtained from one to nine cycles of recycling. It reveals that the compressive and flexural strengths of sand recycled one to three times outperform new sand, while surface hardness remains unaffected by the recycling cycle. However, the permeability of the sand decreases as the number of recycling cycles increases. Recycled sand required less binder and hardener, which reduced costs and improved the environmental impact. This study highlights the importance of waste management and sustainability in 3D-printed sand mold processes and offers a promising solution for recycled sand powders in binder jetting.

**Keywords** Sand casting · Binder jetting · Recycling · Sustainability

## 1 Introduction

Casting, the mother of all industries with a history of over 5000 years, has been facing challenges. This is due to poor working conditions such as high dust, noise, and temperature [1]. To address this issue, the integration of additive manufacturing with casting has become a trend in recent years, offering advantages such as customization, cost savings, and environmental benefits [2–4]. Within the realm of additive manufacturing (AM) techniques, various technology categories exist, including Selective Laser Sintering (SLS), Fused Deposition Modeling (FDM), Fused Filament Fabrication (FFF) and Stereolithography Apparatus (SLA), Digital Light Processing (DLP), Powder Bed Fusion (PBF), among others.

One method of interest is binder jetting (BJ). binder jetting has been found to be the most suitable for sand mold printing. Binder jetting is an additive manufacturing (AM) technology that uses powdered materials like sand, metal, or ceramics. A liquid binder is selectively deposited onto the powder bed via inkjet printing, bonding the particles to form the desired shape. It offers high-resolution, cost-effective, and fast production of complex geometries, making it suitable for prototyping and low-volume production. Its versatility with various materials allows for parts with diverse properties. Several companies, such as ExOne™, Voxeljet™ have developed equipment based on binder jetting technology [5, 6], which involves spraying furan resin onto a powder bed to react with pre-mixed hardener powder and solidify into a sand mold. This technique, similar to traditional furan sand molding, offers comparable mechanical properties with greater precision and less binder usage, resulting in cost savings and environmental benefits [7–11].

Recycling and reusing powder materials are one of the main research topics in the field of additive manufacturing [2, 12]. Many powder materials are used in the other AM technologies, such as stainless steel 316L, AISI 304L, and Ti-6Al-4 V etc. Numerous scholars have studied how to recycle powder

✉ Yen-Ting Li  
saga31110@gmail.com

<sup>1</sup> Department of Mechanical Engineering, National Taiwan University of Science and Technology, No.43, Sec. 4, Keelung Rd., Da'an Dist., Taipei 106, Taiwan, Republic of China

<sup>2</sup> Department of Electrical Engineering, National Tsing Hua University, Hsinchu, Taiwan

to save costs and investigated the impact of recycled powder on mechanical properties [12–17]. A study [18] that examined the influence of reusing powder on the characteristics of Ti-6Al-4 V powder, including the powder's physical properties such as composition, particle size distribution (PSD), apparent density, tap density, flowability, and particle morphology, found that the repeated use of powder-based materials has no adverse effects on the AM process, and the testing samples exhibited highly consistent tensile properties. In addition to metal powders, Nicole E. Zander ' team proposed the idea of processing and reusing waste PET, PP, ABS, PLA, and PS materials [19–23]. Although additive manufacturing already has advantages such as material efficiency, environmental friendliness, and cost savings over traditional processes, numerous scholars still hope that this technology can be more environmentally friendly and reduce material waste [24–31].

The use of 3D-printed sand molds with furan resin is still in its nascent stages, with much research focused on shell design [7, 32–35], mechanical properties [36–38], and more precise core printing [40–42]. However, there has been increasing attention paid to the issue of sustainability in sand mold casting, with scholars exploring topics such as energy efficiency and CO<sup>2</sup> emissions in foundries [42–45], as well as alternative resins and hardeners [46–48]. The impact of sand waste and dust on the environment has also been studied [49, 50]. While binder jetting is still less prevalent in the traditional foundry industry [51–54], many current binder jetting studies use new sand powders, and nearly all waste sand that has been binder-jetted or used in casting is treated as disposable waste [55]. This differs from traditional furan molding, where used sand is typically processed and reused until it is worn down to dust. Given this, it is essential to address waste management and environmental concerns in binder jetting processes if we want to achieve sustainability goals.

This study aims to tackle the waste management issue by demonstrating that recycled sand can produce mechanical properties comparable to, if not better than, those of new sand. To do so, we designed an experimental procedure that mimicked the processing of waste sand in traditional furan molding, and used it to measure properties such as compressive and bending strength, surface hardness, permeability, and molding accuracy. The results showed that the mechanical properties of recycled sand were not significantly different from those of new sand and, in some cases, exceeded them. Additionally,

the amount of binder and hardener used in recycled sand was significantly less than that required for new sand, resulting in cost savings and environmental benefits.

In conclusion, this study emphasizes the importance of waste management and sustainability in 3D-printed sand mold processes, and provides a promising solution for recycled sand powders in binder jetting. By demonstrating the comparable mechanical properties of recycled sand, we have shown that waste sand can be a valuable resource that, when managed effectively, can significantly reduce waste and environmental impact.

## 2 Materials and experimental methods

### 2.1 Materials

Furan sand casting, also known as resin sand casting, is a method of sand casting. This method utilizes furan resin as a binding agent and mixes it with a catalyst (hardening agent) in adequate proportions to produce sand molds. The type of furan sand casting being discussed is self-hardening, which means that the sand mold does not require curing; instead, it hardens itself at room temperature. For this experiment, we used silicon sand with a particle size range of 70–200 μm, commonly used in sand casting, and mixed with 3 wt% of a hardening agent. K.L.CHEMICALS CO., LTD. provided us with furan resin as a binder, with a density of 2.34 g/cm<sup>3</sup>, and a viscosity of 14.55 cp as measured by a US BROOKFIELD viscometer DV2T, with a surface tension of 40.23 mN/m and a contact angle of 130°, as measured by Model 100SB and NBSI OSA60, respectively. All measurements were conducted at room temperature (24.5 °C) and the average values were obtained after five repetitions, as shown in Table 1.

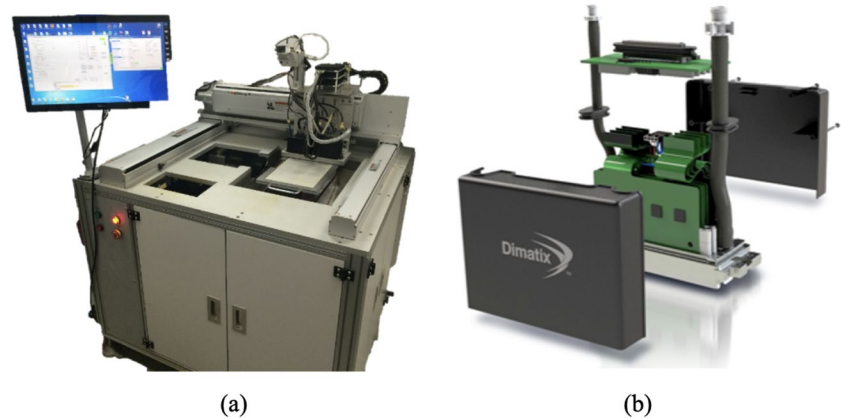
### 2.2 Experiment

In this study, a custom-built binder jetting printer was employed, as depicted in Fig. 1a The printer has dimensions of 1170 mm × 1100 mm and offers a printing spatial range of 200 mm (l) × 300 mm (w) × 200 mm (h). It utilizes three-axis motion, with three Fujifilm SG1024 (Fig. 1b) piezoelectric printheads positioned on the X-axis. Each printhead comprises

**Table 1** Parameters

Sand particles					
Density(g/cm <sup>3</sup> )	Particle size(um)	Porosity(%)	D <sub>10</sub>	D <sub>50</sub>	D <sub>90</sub>
2.594	70–200	38.2	122.8	201.9	296.0
Binder (Furan resin)					
Surface Tension(mN/m)			Viscosity (cP)		
40.23			14.55		

**Fig. 1** The experimental setup consists of the Sand Molding Machine shown in (a), which utilizes a printhead Fujifilm SG1024, as depicted in (b)



1024 independent channels in 8 rows within a single nozzle plate, enabling single color operation at 400 dpi. The printhead which is compatible with the furan resin used in this study and can print at a speed of 7 cm/s. The binder volume was controlled by adjusting the drive voltage and waveform [56, 57], and the calculated single binder volume was 13.6  $\mu\text{L}$ . The printer's nominal fluid viscosity ranges from 8–20 cP (10–14 cP recommended by the vendor), and the inkjet operating temperature can go up to 50 °C (122°F). The machine includes a sand paver for 0.3 mm layer spreading, a liquid binder supply, and a user interface touch panel. For this research, Furan resin served as the binder, and the powder consisted of silica particles. The SG1024 printhead is capable of injecting Furan resin at a droplet injection velocity typically ranging from 1.9 m/sec to 3.2 m/sec, as measured using a high-speed camera.

We started with fresh sand (test A) and conducted common sand casting tests and mechanical tests such as compressive strength, flexural strength, surface hardness, air permeability, and dimensional accuracy. After the measurements, the samples were baked in an AKT-814ALKEMT Co Ltd high-temperature furnace at 100 °C for 30 min to remove moisture and then at 1000 °C for 20 min to simulate the heat exposure during casting. However, some of the sand particles were still bonded by the resin. Therefore, we used a sand grinder to crush the sand and obtained the treated secondary sand (no additional chemical treatment was necessary as the furan resin and hardening agent were the only additives in the furan sand mold). We mixed the used secondary sand with fresh sand in a 95%:5% ratio (the same as the traditional furan sand mold factory's processing method) to obtain test B. We repeated the sand casting tests and mechanical tests on test B, and after baking, sintering, and crushing, we mixed 95% of the treated secondary sand with 5% of fresh sand to obtain test C. We repeated these steps ten times to obtain tests A to J, to investigate the recycling rate of waste sand in binder jetting. The measurement methods and equipment used for mechanical properties are listed in order below.

### 2.2.1 Compressive strength

To evaluate the compressive strength, we used the SCST-520 ALKEMT Co Ltd (as shown in Fig. 2a). Samples with a diameter of 50 mm and a height of 50 mm were printed, as shown in Fig. 2b. Sand compression test evaluates the mechanical properties of foundry sand by subjecting a cylindrical sample to uniaxial compressive load until it fractures, providing crucial data for mold-making and casting applications. Each mixture ratio was tested in triplicate, and after 24 h of curing, the compressive strength was measured.

### 2.2.2 Flexural strength

To measure the flexural strength, we also used the SCST-520 ALKEMT Co Ltd. (as shown in Fig. 2a) machine, following the ASTM B312 standard, as shown in Fig. 2c. The three-point bending test evaluates the flexural strength and stiffness of materials by applying a load at two points while supporting the specimen at its center, offering insights into their mechanical performance and structural behavior. Each mixture ratio was tested in triplicate, and after 24 h of curing, the flexural strength was measured.

### 2.2.3 Hardness test

The surface hardness of the samples was measured using the same samples used for compressive strength and permeability tests. We used the Surface hardness tester AKT-807 ALKEMT Co Ltd (as shown in Fig. 3a). This method involves using a hardness tester with a probe that applies pressure to the surface of the specimen. As the probe is pressed into the material, the hardness tester's indicator needle rotates, allowing us to determine the hardness value of the surface. Each mixture ratio was printed in triplicate, and three points were measured and averaged for each sample.

**Fig. 2** The strength of the printed samples was assessed using common foundry tests (a), including compressive strength, flexural strength

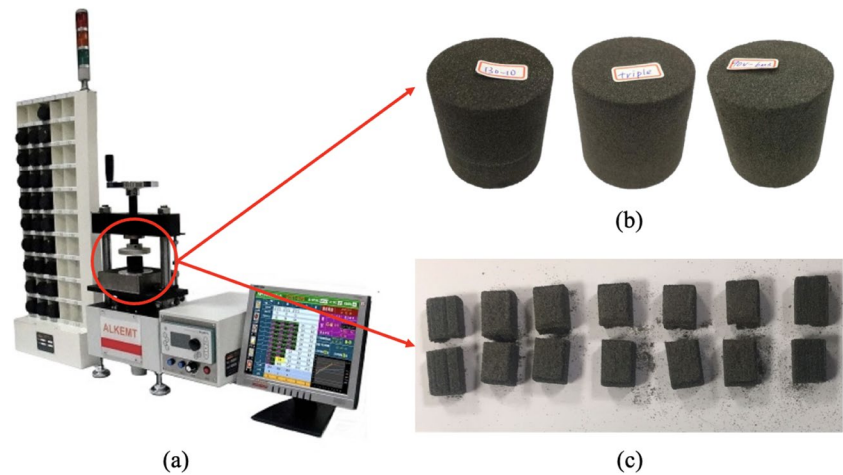
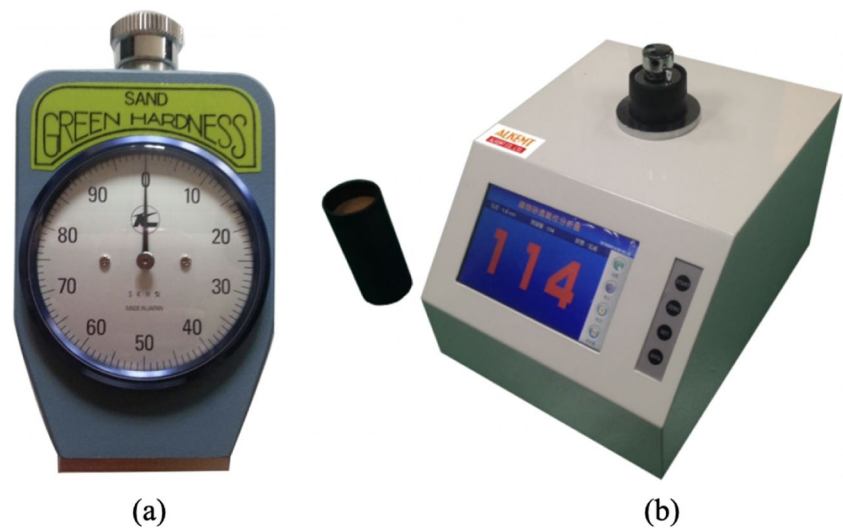


**Fig. 3** The surface hardness tester AKT-807 in (a), and AKT-816 in (b)



#### 2.2.4 Permeability

To measure the permeability, we printed five samples with a diameter of 50 mm and a height of 50 mm, and used the Permeability tester AKT-816 ALKEMT Co Ltd. (as shown in Fig. 3b.) The sand permeability test measures the gas flow rate through a sand sample to evaluate its ventilation performance during the casting process. Since the samples used for permeability and compressive strength tests were the same, we conducted the permeability test before the compressive strength test. Each mixture ratio was tested in triplicate.

#### 2.2.5 Dimension error

The layer thickness used in our machine is 0.3 mm, which makes it difficult to measure in a single layer. Therefore, we printed four samples with a dimension of 30 mm (*l*) x 30 mm (*w*) x 6 mm (*h*), as shown in Fig. 4. We used a vernier caliper to measure three points and averaged the

values to obtain the size, subtracting the original design size to obtain the size overflow. We measured the size overflow in both horizontal and vertical directions. Since different printing directions have different size errors, we considered the size overflow in the printing and non-printing directions in the horizontal direction. As some mechanical properties can be measured using samples with the same geometric shape, we listed the printed sample geometries and corresponding tests in Table 2.

#### 2.2.6 Loss on ignition (LOI)

We placed the samples in the AKT-814 ALKEMT Co Ltd high-temperature furnace, as shown in Fig. 5a, for baking. The samples were first baked at 100°C for 30 min to remove moisture, followed by baking at 1000°C for 90 min to burn off all binders. (as shown in Fig. 5b.) We then calculated the initial binder content  $V_{binder}$ , which was 1.5 g, by comparing the weight difference before and after combustion and dividing it by the weight of the original powder.

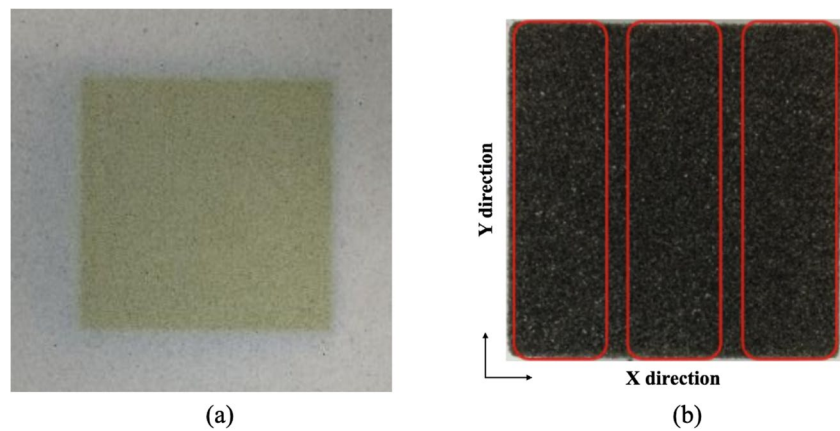


### 3 Results and discussion

Additive manufacturing technology has different strengths in different printing directions, as noted in [46]. In our research, we printed data in the direction that resulted in the highest strength. After sintering, we used a Dino-Lite Premier AM4113T5X microscope with Media Cybernetics Image-Pro 10 software to analyze the particle size distribution of the recycled sand. We found that the particle size decreased by about  $3.2 \pm 1.2\%$  of the original size. Initially, the new sand had a polygonal shape, which is ideal for casting [58], but after sintering, the shape became more rounded, as shown in Fig. 6a. As the sintering and rolling cycles increase, numerous tiny particles and dust are generated as shown in Fig. 6b. These particles have a detrimental effect on the mechanical properties of the sand mold. To reduce the amount of binder and hardener used,

we followed the traditional furan mold method and determined the optimal mixing ratio by analyzing the LOI experimental results. We adjusted the waveform to ensure that the binder saturation in each sample was the same with a saturation error of approximately 10%. Previous studies have shown that using smaller sand particles results in better dimensional accuracy and mechanical properties [39, 40, 42]. However, as the silica sand is repeatedly sintered, the particle size distribution changes. Tests A, D, G, and H in our research represent different particle size distributions, with test A being a single-peak sand and tests D, G, and H being bimodal distributions. As the sand is repeatedly sintered, the peak height decreases. Furthermore, as shown in Fig. 6b, the proportion of dust and fine particles in the sand increases with repeated sintering, which can pose a health and environmental hazard for the operators. Upon careful observation, clear bimodal peaks are evident in Test D and G,

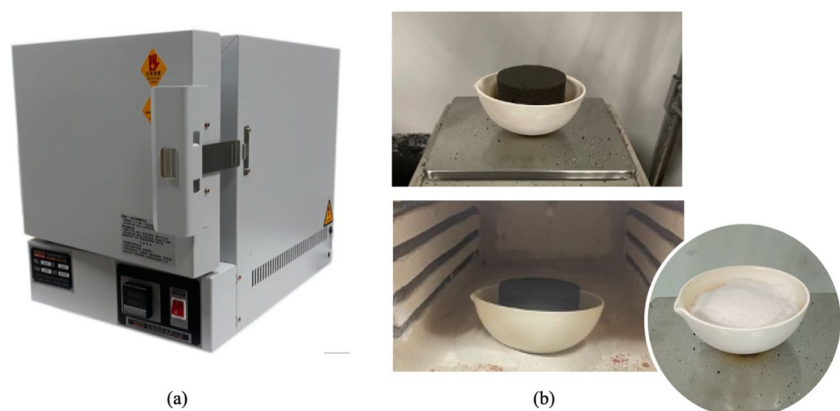
**Fig. 4** The sample's dimensions were measured to be 30 mm (l) x 30 mm (w) x 6 mm (h)



**Table 2** Geometry of tests

	Geometry 1	Geometry 2	Geometry 3
Dimensions	Ø50 mm x 50 mm (l)	31.7 mm x 12.7 mm x 6.35 mm	30 mm (l) x 30 mm (w) x 6 mm (h)
Measurement	Permeability Compressive strength	Flexural strength	Dimension error Hardness test

**Fig. 5** The LOI tester AKT-814 in (a). (b) shows a comparison before and after placing the sample in the oven. The green-colored resin completely disappears after baking, revealing the original color of the silica sand (white). By comparing the weight difference before and after baking, we can determine the weight of the resin



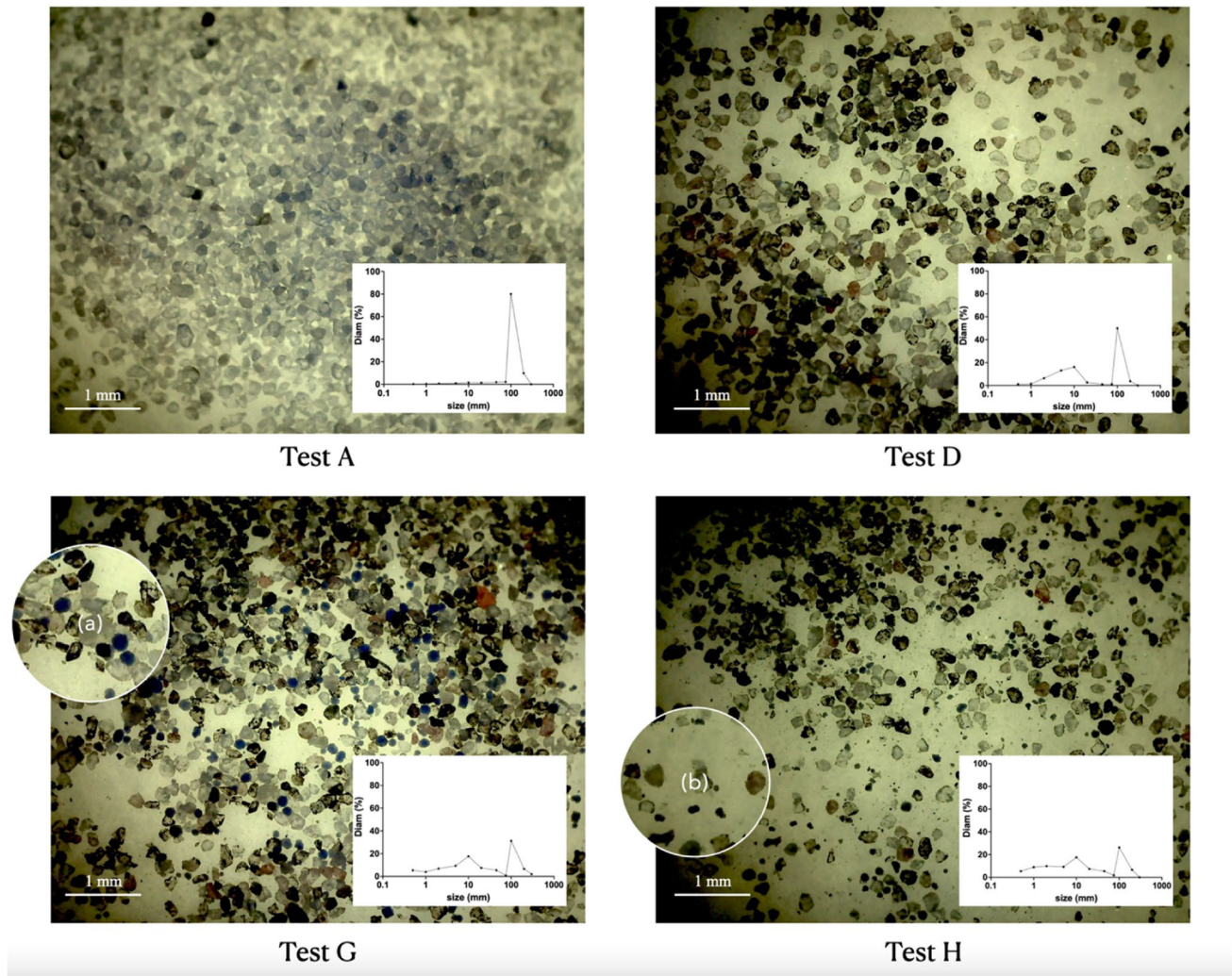


**Fig. 6** The particle size analysis and distribution of test A, D, G and H were captured using a microscope

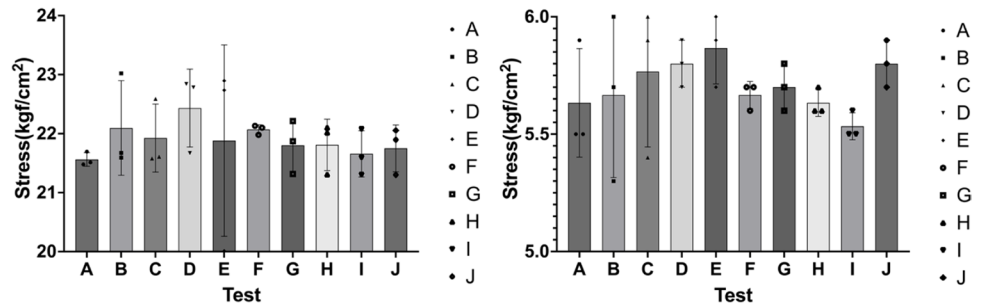
which is beneficial for furan casting as it indicates the presence of smaller particles within the larger ones, leading to a more complete reaction between furan resin and hardener, resulting in improved dimensional accuracy and surface smoothness of the sand mold. However, in Test G and H, the bimodal peaks begin to decrease, and other particle sizes start to emerge, indicating that with an increasing number of repeated sintering cycles, the particle distribution becomes more chaotic. While bimodal peaks are still apparent, the additional particles generated can negatively impact the properties of the sand mold.

### 3.1 Compressive strength

Regarding the compressive strength results, refer to Fig. 7a. Under the same binder volume, tests B to D perform the best, while the strength of pure new sand is similar to tests E to J, which is expected. In traditional furan resin casting, the best molding effect is not achieved using the commonly used

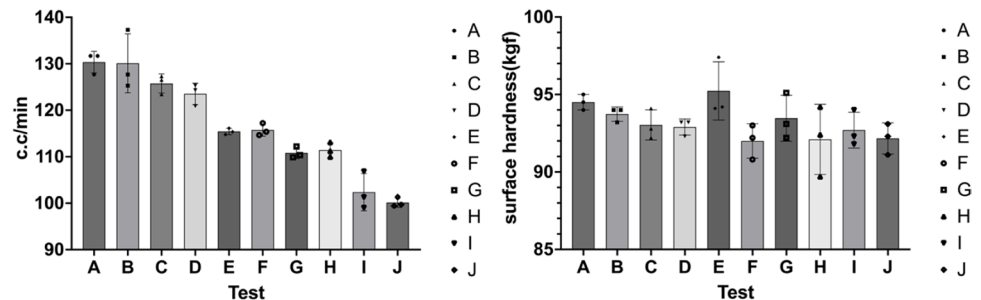
$D_{30}$  or  $D_{50}$  single-peak effective particle size, but by using bimodal or trimodal distributions [36, 57]. This means that there are smaller particles covered in larger sand particles. This result is the same as traditional furan resin molding, which also uses sand with a particle size analysis of bimodal to trimodal distribution, to obtain the best compressive strength. Small sand particles can fill the pores between larger particles, making the sand mold more compact, increasing the contact area between the binder and powder hardener, and having a higher strength while also having a better reaction efficiency [57]. Interestingly, the error of tests B to E is larger in the graph, while the error of tests A and F to J is smaller. We believe this is due to the sample sampling. For example, in tests B to E, two of the three samples have the same stress values measured, while the other has a larger difference, which also occurs in other tests. In the compressive strength test, as soon as the sample is cracked under pressure, it is considered to have reached its maximum strength.

**Fig. 7** Comparison of mechanical properties by using recycled sand and new sand



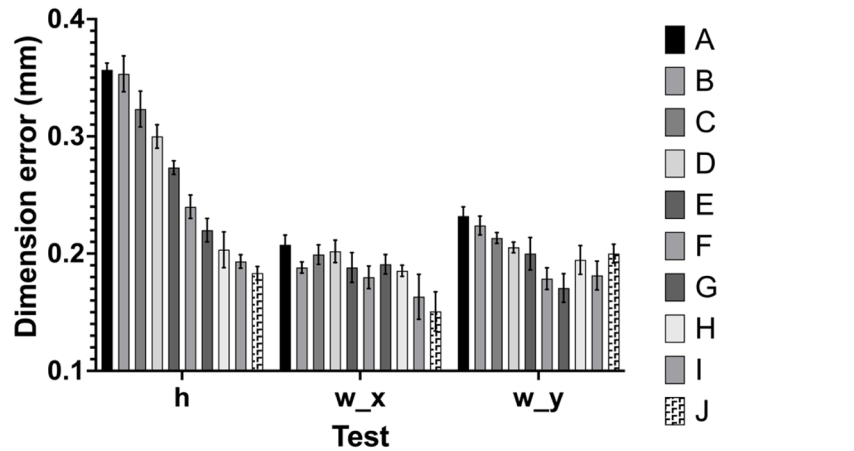
(a) Compressive strength

(b) Flexural strength



(c) Permeability

(d) Surface hardness



(e) Dimension error

### 3.2 Flexural strength

Similar to compressive strength, different powder mixing ratios also have different flexural strengths as shown in Fig. 7b. However, overall, the differences in performance between the tests appear to be small, all falling within the range of 5.4–5.8 kgf/cm<sup>2</sup>. But, in general, flexural strength is not proportional to compressive strength, which can be explained by the fact that during flexural strength testing, the upper part of the sample is subjected to compressive stress while the lower part is subjected to tensile stress. Binder jetting’s tensile strength on sand molding is far inferior to its compressive strength, which causes the

binding force between the powder and binder to decrease and the flexural strength performance to be less outstanding than the compressive strength. Since the sand mold needs to withstand the weight of the casting, compressive strength is more important than flexural strength.

### 3.3 Permeability

The performance of permeability can be referred to in Fig. 7c. Permeability is related to porosity, with larger porosity resulting in better permeability. If the porosity is large, the binder does not completely fill the gaps between the powders when



infiltrating the powder bed, making it easier for gas to pass through and making the permeability better [59, 60]. As recycled sand is repeatedly sintered, its size gradually decreases, making the porosity smaller and the permeability gradually worse. Generally, the permeability of furan molds is between 110–130 c.c./min [58], so tests A–H can all meet the standard of permeability of a typical furan mold, with A–D having better permeability. Conversely, the permeability performance of tests I and J is significantly worse than that of other tests because the sand grains have been repeatedly sintered and crushed many times, resulting in many extremely small particles that are approaching the size of dust. These particles have a significant negative impact on permeability. Especially in sand core production, unlike sand molds where risers and vents can be designed, the permeability of sand cores can avoid the high-temperature impact of casting and prevent the sand core from cracking.

### 3.4 Hardness test

The performance of surface hardness can be referred to in Fig. 7d. Although the performance of test F is worse than that of other tests, the overall difference is less than 5 kgf, indicating that there is not much relationship between surface hardness and the mixing ratio of sand. Another interesting comparison is that the error value of surface hardness is higher than that of other mechanical properties. This is because surface hardness is determined by a probe applying force to the surface of the object, which is composed of powder and binder. The location where the probe is pressed may not necessarily be on the binder or on the powder, resulting in a larger error. This is also why the differences in surface hardness are not significant between the tests. However, the overall surface hardness of all tests, regardless of which test it is, cannot be determined by the data chart.

### 3.5 Dimension error

In terms of dimensional error, it can be seen in Fig. 7e that the dimensional errors of all tests are within the range of  $\pm 0.3\%$ , which meets the requirements of general precision casting. The dimensional error of test F is slightly higher, which may be related to the mixing ratio of sand or the printing accuracy of the 3D printer. Overall, the dimensional accuracy of binder jetting sand molds is high, which can effectively reduce the machining allowance of castings and improve production efficiency.

## 4 Possibility of reusing sand and reduction of consumables

In this study, we discuss the method proposed to reuse sand and reduce the consumption of consumables. The experimental results have shown that the use of recycled sand has

little impact on mechanical properties, except for a decrease in permeability with increasing sintering and grinding cycles. In fact, some mechanical properties have performed better than new sand. Next, we compared the reduced consumption of consumables and the usage of recycled sand with new sand in terms of test A compressive strength of the  $\text{Ø}50 \text{ mm} \times 50 \text{ mm}$  (I) sample.

### 4.1 Usage of recycled sand

The amount of silica sand used in test A compressive strength of  $\text{Ø}50 \text{ mm} \times 50 \text{ mm}$  (I) is  $81.1 \pm 0.73 \text{ g}$ . After each sintering, 95% of the sand, approximately 77.045 g, is reused with an additional 5%, approximately 4.055 g of new sand added for test B. This process is repeated ten times, from test A to J. If new sand is used for all ten tests, the amount of silica sand used is  $811 \pm 7.3 \text{ g}$ . However, if recycled sand is reused, the amount of silica sand used is approximately 117.595 g, which is 6.87 times less than using new sand. Therefore, using recycled sand can save costs and is more environmentally friendly than using pure new sand.

### 4.2 Reduction of binder

As recycled sand contains partially bound binder and unreacted hardener, less binder can be used when printing with recycled sand compared to new sand. In this study, a piezoelectric nozzle was used to spray a single binder volume of 13.6  $\mu\text{L}$ . After printing test A and sintering, the initial  $V_{\text{binder}}$  content was found to be 1.5 g. Since there is residual binder left in the sample after each sintering, as shown in Fig. 4, we do not need to use a 13.6  $\mu\text{L}$  volume of binder for printing. By adjusting the waveform [56], we tested 8.1, 9.5, and 11.4  $\mu\text{L}$  for printing. However, 8.1  $\mu\text{L}$  was too small to fully cure, and 11.4  $\mu\text{L}$  resulted in binder saturation. Therefore, we used 9.5  $\mu\text{L}$  for printing test B to J. We performed LOI sintering on each sample that underwent compressive strength testing and calculated the amount of binder used for each test, as well as the amount added each time, which is presented in Fig. 8a.

The initial  $V_{\text{binder}}$  1.5 g was divided by the silica sand weight 81.1 g and converted to a percentage, resulting in a binder addition rate of 1.85%. If we subtract the binder increase of 1.04 g (converted using 9.5  $\mu\text{L}$ ) used in tests B to J from the initial  $V_{\text{binder}}$  1.5 g, the binder addition rate is reduced to 0.57%. This means that the use of recycled sand and new sand will result in a difference of about 1.3% in binder usage for each sand mold printed.

### 4.3 Reduction of hardener

Sand grains used in binder jetting are smaller than those in traditional furan molds, resulting in an increased



surface area per unit volume of powder. Consequently, the required hardener content in the market is approximately 3 wt%, compared to the 1 wt% required for traditional furan molds. Reducing the hardener content not only decreases cost but also minimizes the negative environmental impact of the hardener.

Through each repeated cycle of sintering, grinding, and reprinting, the necessary hardener content can be reduced by approximately 0.3 wt%, a trend that persists until test E. However, we have observed that the curing time lengthens after test E, likely due to an insufficient hardener content. As sand particles become pulverized, they produce numerous small particles or dust, increasing the contact surface area and necessitating a higher hardener content. To maintain the curing time at the same level as that of new sand, we present the required hardener usage per cycle in Fig. 8b.

### 5 Conclusion

Through mechanical property experiments, this study demonstrated that using recycled sand does not result in inferior performance compared to using pure new sand, especially in terms of compressive strength and flexural strength. Tests B to D even showed slightly superior results compared to pure new sand (Test A). There was no significant difference in surface hardness between new and recycled sand. However, the more recycled sand was used, the more particles and dust accumulated, leading to poor air permeability. In terms of dimensional accuracy, the use of recycled sand performed slightly better in vertical accuracy but similar to new sand in horizontal accuracy.

Furthermore, the results presented in this study still require further validation through practical experiments to confirm the effectiveness of using recycled sand in 3D printing. The actual casting process may differ slightly from the experimental setup in this study, as real-world casting often involves phenomena like burning and erosion due to molten metal injection, which could cause more significant damage to the sand mold and hinder its recyclability.

During the experiment, the recycled sand underwent slight changes in particle morphology after the sintering process, transitioning from polygonal particles suitable for casting to more rounded ones due to repeated wear. While this difference in particle shape could potentially affect the bulk density, its impact on the results was not substantial. This is because 3D-printed sand molds do not involve compacting actions, resulting in minimal variation in bulk density.

The primary concern of this study was to compare the mechanical properties between old and new sand and investigate the usage of silica sand, binder, and hardener. After ten printing tests, the use of recycled sand resulted in a maximum reduction of up to six times the amount of new sand used, 1.3% less binder, and approximately 1.2 wt% less hardener. Although using recycled sand is more environmentally friendly and cost-effective, this study suggests that recycled sand should be replaced after being reused three to four times (i.e., Tests B-E). The best compressive strength and flexural strength performances were observed in this range, with air permeability still similar to new sand. As the number of sintering and grinding repetitions increases, the amount of particles and dust increases, leading to reduced air permeability and unstable printing processes. Excessive particles and dust also have negative effects on the environment and users' health. Therefore, although recycled sand can replace some new sand, the reuse frequency should not be excessive.

Furthermore, this study still requires more experiments and even practical applications to confirm the difference

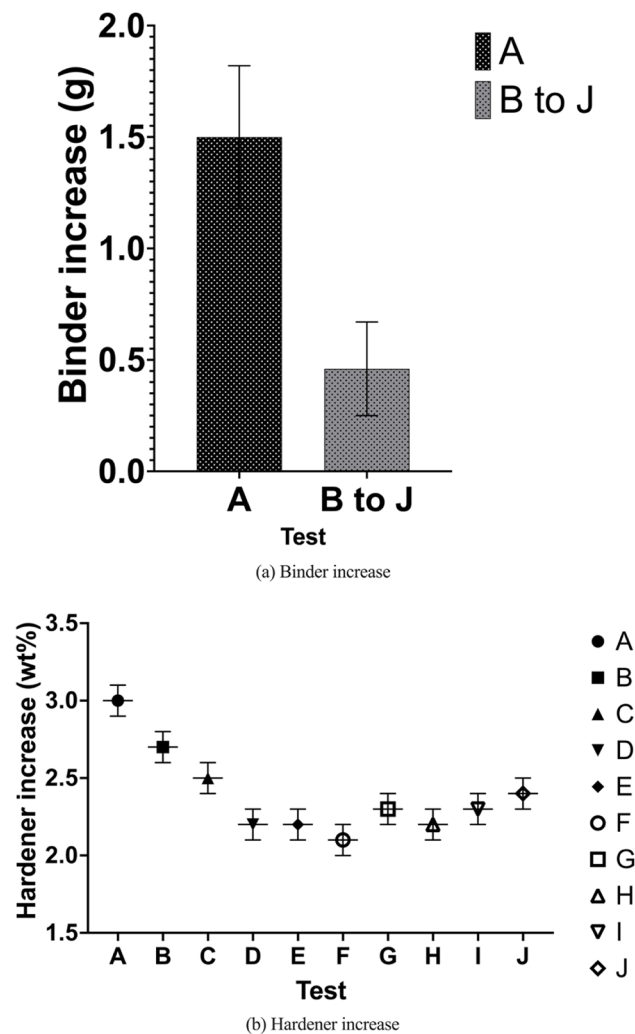


Fig. 8 The binder and hardener used for each sample

between old and new sand. This study serves as a preliminary experiment to raise the issue of reusing recycled sand and hopes to achieve a good balance between technology and environmental conservation.

#### Author contribution

Author	Name	Term
Author 1	Yen-Ting Li	Conceptualization, Validation, Methodology, Writing—Original Draft, Review & Editing
Author 2	Yih-Lin Cheng	Conceptualization, Supervision
Author 3	Kea-Tiong Tang	Resources, Supervision

**Funding** This research project did not receive any specific grant from funding agencies in the public, commercial, or not-for-profit sectors.

**Data availability** Data will be made available on request.

#### Declarations

**Competing interest** The authors declare that they have no known competing financial interests or personal relationships that could have appeared to influence the work reported in this paper.

#### References

- Salonitis K, Zeng B, Mehrabi HA, Jolly M (2016) The challenges for energy efficient casting processes. *Procedia CIRP* 40:24–29. <https://doi.org/10.1016/j.procir.2016.01.043>
- Upadhyay M, Sivarupan T, Mansori ME (2017) 3D printing for rapid sand casting—a review. *J Manuf Process* 29:211–220. <https://doi.org/10.1016/j.jmapro.2017.07.017>
- Hawalder N, Zhang J (2018) A comparative study of fabrication of sand casting mold using additive manufacturing and conventional process. *Int J Adv Manuf Technol* 97:1037–1045. <https://doi.org/10.1007/s00170-018-2020-z>
- Gill SS, Kaplas M (2011) Efficacy of powder-based three-dimensional printing (3DP) technologies for rapid casting of light alloys. *Int J Adv Manuf Technol* 52:53–64. <https://doi.org/10.1007/s00170-010-2716-1>
- Voxeljet (2023) <https://www.voxeljet.com/>. Accessed 25 Aug 2023
- Exone (2023) <https://www.exone.com/en-US>. Accessed 25 Aug 2023
- Kang J, Shangguan H, Deng C, Hu Y, Yi J, Wang X, Zhang X, Huang T (2018) Additive manufacturing-driven mold design for castings. *Addit Manuf* 22:472–478. <https://doi.org/10.1016/j.addma.2018.04.037>
- Gill SS, Kaplas M (2009) Comparative study of 3D printing technologies for rapid casting of aluminium alloy. *Mater Manuf Processes* 224:1405–1411. <https://doi.org/10.1080/10426910902997571>
- Singamneni S, McKenna N, Diegel O, Singh D, Neitzert T, George JS, Choudhury AR, Yarlaga P (2009) Rapid casting: a critical analysis of mould and casting characteristics. *Aust J Mech Eng* 7:33–43. <https://doi.org/10.1080/14484846.2009.11464576>
- Coniglio N, Sivarupan T, El Mansori M (2018) Investigation of process parameter effect on anisotropic properties of 3D printed sand molds. *Int J Adv Manuf Technol* 94:2175–2185. <https://doi.org/10.1007/s00170-017-0861-5>
- Ramakrishnan R, Griebel B, Volk W, Günther D, Günther J (2014) 3D printing of inorganic sand moulds for casting applications. *AMR* 1018:441–449. <https://doi.org/10.4028/www.scientific.net/amr.1018.441>
- Le T, Wang X, Seita M (2022) An optical-based method to estimate the oxygen content in recycled metal powders for additive manufacturing. *Addit Manuf* 59(Part A):103127. <https://doi.org/10.1016/j.addma.2022.103127>
- Delacroix T, Lomello F, Schuster F, Maskrot H, Garandet J (2022) Influence of powder recycling on 316L stainless steel feedstocks and printed parts in laser powder bed fusion. *Addit Manuf* 50:102553. <https://doi.org/10.1016/j.addma.2021.102553>
- He X, Kong D, Zhou Y, Wang L, Ni X, Zhang L, Wu W, Li R, Li X, Dong C (2022) Powder recycling effects on porosity development and mechanical properties of Hastelloy X alloy during laser powder bed fusion process. *Addit Manuf* 55:102840. <https://doi.org/10.1016/j.addma.2022.102840>
- Maamoun AH, Elbestawi M, Dosbaeva GK, Veldhuis SC (2018) Thermal post-processing of AlSi10Mg parts produced by selective laser melting using recycled powder. *Addit Manuf* 21:234–247. <https://doi.org/10.1016/j.addma.2018.03.01>
- Sutton AT, Kriewall CS, Karnati S, Leu MC, Newkirk JW, Everhart W, Brown B (2020) Evolution of AISI 304L stainless steel part properties due to powder recycling in laser powder-bed fusion. *Addit Manuf* 36:101439. <https://doi.org/10.1016/j.addma.2020.101439>
- Sutton AT, Kriewall CS, Karnati S, Leu MC, Newkirk JW (2020) Characterization of AISI 304L stainless steel powder recycled in the laser powder-bed fusion process. *Addit Manuf* 32:100981. <https://doi.org/10.1016/j.addma.2019.100981>
- Tang HP, Qian M, Liu N, Zhang XZ, Yang GY, Wang J (2015) Effect of powder reuse times on additive manufacturing of Ti-6Al-4V by selective electron beam melting. *JOM* 67:555–563. <https://doi.org/10.1007/s11837-015-1300-4>
- Zander NE, Gillan M, Burckhard Z, Gardea F (2019) Recycled polypropylene blends as novel 3D printing materials. *Addit Manuf* 25:122–130. <https://doi.org/10.1016/j.addma.2018.11.009>
- Solodov AN, Shayimova J, Balkaev D, Nizamutdinov AS, Zimin K, Kiiamov AG, Amirov RR, Dimiev AM (2022) High-throughput, low-cost and “green” production method for highly stable polypropylene/perovskite composites, applicable in 3D printing. *Addit Manuf* 59(Part A):103094. <https://doi.org/10.1016/j.addma.2022.103094>
- Singh P, Katiyar P, Singh H (2023) Impact of compatibilization on polypropylene (PP) and acrylonitrile butadiene styrene (ABS) blend: A review. *Materials Today: Proc* 78(Part 1):189–197. <https://doi.org/10.1016/j.matpr.2023.01.350>
- Liu Q, Zhang X, Jia D, Yin J, Lei J, Xu L, Lin H, Zhong G, Li Z (2023) In situ nanofibrillation of polypropylene/polyethylene/poly(ethylene terephthalate) ternary system: a strategy of upgrade recycling. *Polymer* 269:125729. <https://doi.org/10.1016/j.polymer.2023.125729>
- Giani N, Mazzocchetti L, Benelli T, Picchioni F, Giorgini L (2022) Towards sustainability in 3D printing of thermoplastic composites: Evaluation of recycled carbon fibers as reinforcing agent for FDM filament production and 3D printing. *Compos Part A: Appl Sci Manuf* 159:107002. <https://doi.org/10.1016/j.compositesa.2022.107002>

24. Peng T, Kellens K, Tang R, Chen C, Chen G (2018) Sustainability of additive manufacturing: an overview on its energy demand and environmental impact. *Addit Manuf* 21:694–704. <https://doi.org/10.1016/j.addma.2018.04.022>
25. de Voorde BV, Katalagarianakis A, Huysman S, Toncheva A, Raquez J, Duretek I, Holzer C, Cardon Ludwig, Bernaerts KV, Hemelrijck DV, Pyl L, Vlierberghe SV (2022) Effect of extrusion and fused filament fabrication processing parameters of recycled poly(ethylene terephthalate) on the crystallinity and mechanical properties. *Addit Manuf* 50:102518. <https://doi.org/10.1016/j.addma.2021.102518>
26. Mohammed M, Wilson D, Gomez-Kervin E, Petsiuk A, Dick R, Pearce JM (2022) Sustainability and feasibility assessment of distributed E-waste recycling using additive manufacturing in a Bi-continent context. *Addit Manuf* 50:102548. <https://doi.org/10.1016/j.addma.2021.102548>
27. Chandrasekar S, Coble JB, Yoder S, Nandwana P, Dehoff RR, Paquit VC, Babu SS (2020) Investigating the effect of metal powder recycling in electron beam powder bed fusion using process log data. *Addit Manuf* 32:100994. <https://doi.org/10.1016/j.addma.2019.100994>
28. Zander NE, Gillan M, Lambeth RH (2018) Recycled polyethylene terephthalate as a new FFF feedstock material. *Addit Manuf* 21:174–182. <https://doi.org/10.1016/j.addma.2018.03.007>
29. Hart KR, Frketic JB, Brown JR (2018) Recycling meal-ready-to-eat (MRE) pouches into polymer filament for material extrusion additive manufacturing. *Addit Manuf* 21:536–543. <https://doi.org/10.1016/j.addma.2018.04.011>
30. Fateri M, Kaouk A, Cowley A, Siarow S, Palou MV, González FG, Marchant R, Cristoforetti S, Sperl M (2018) Feasibility study on additive manufacturing of recyclable objects for space applications. *Addit Manuf* 24:400–404. <https://doi.org/10.1016/j.addma.2018.09.020>
31. Byard DJ, Woern AL, Oakley RB, Fiedler MJ, Snabes SL, Rearece JM (2019) Green fab lab applications of large-area waste polymer-based additive manufacturing. *Addit Manuf* 27:515–525. <https://doi.org/10.1016/j.addma.2019.03.006>
32. Shangguan H, Kang J, Deng C, Hu Y, Huang T (2017) 3D-printed shell-truss sand mold for aluminum castings. *J Mater Process Technol* 250:247–253. <https://doi.org/10.1016/j.jmatprotec.2017.05.010>
33. Shangguan H, Kang J, Yi J, Zhang X, Wang X, Wang H, Huang T (2018) The design of 3D-printed lattice-reinforced thickness-varying shell molds for castings. *Materials* (Basel, Switzerland) 11:535. <https://doi.org/10.3390/ma11040535>
34. Shangguan H, Kang J, Yi J, Deng C, Hu Y, Huang T (2018) Controlled cooling of an aluminum alloy casting based on 3D printed rib reinforced shell mold. *China Foundry* 15:210–215
35. Deng C, Kang J, Shangguan H, Hu Y, Huang T, Liu Z (2018) Effects of hollow structures in sand mold manufactured using 3D printing technology. *J Mater Process Technol* 255:516–523. <https://doi.org/10.1016/j.jmatprotec.2017.12.031>
36. Hu C, Du W (2018) Research on the method for improving mechanical properties of sand mold based on 3D printing process. *IOP Conf Ser Mater Sci Eng* 394(3):032063. <https://doi.org/10.1088/1757-899X/394/3/032063>
37. Sivarupan T, Mansori ME, Coniglio N, Dargusch M (2020) Effect of process parameters on flexure strength and gas permeability of 3D printed sand molds. *J Manuf Process* 54:420–437. <https://doi.org/10.1016/j.jmapro.2020.02.043>
38. Sivarupan T, Mansori ME, Daly K, Mavrogordato MN, Pierron F (2019) Characterisation of 3D printed sand moulds using micro-focus X-ray computed tomography. *Rapid Prototyp J* 25(2):404–416. <https://doi.org/10.1108/RPJ-04-2018-0091>
39. Polmear I, StJohn D, Nie JF, Qian M (2017) Casting of light alloys. In: Polmear I, StJohn D, Nie JF, Qian M (eds) *Light Alloys*. Butterworth-Heinemann, Boston, pp 109–156
40. Almaghariz ES, Conner BP, Lenner L, Gullapalli R, Manogharan GP, Lamoncha B, Fang M (2016) Quantifying the Role of Part Design Complexity in Using 3D Sand Printing for Molds and Cores. *Inter Metalcast* 10:240–252. <https://doi.org/10.1007/s40962-016-0027-5>
41. Wang J, Qu A, Langlois TR, James DL (2018) Toward wave-based sound synthesis for computer animation. *ACM Trans Graph* 37(4):1–16. <https://doi.org/10.1145/3197517.3201318>
42. Sivarupan T, Balasubramani N, Saxena P, Nagarajan D, Mansori ME, Salonitis K, Jolly M, Dargusch MS (2021) A review on the progress and challenges of binder jet 3D printing of sand moulds for advanced casting. *Addit Manuf* 40:101889. <https://doi.org/10.1016/j.addma.2021.101889>
43. ENERGETICS, Inc (2017) *Energy and Environmental Profile of the U.S. Aluminum Industry*, Columbia, Maryland, USA
44. Sa A, Paramonova S, Thollander P, Cagno E (2015) Classification of industrial energy management practices. *Energy Procedia* 75:2581–2588. <https://doi.org/10.1016/j.egypro.2015.07.311>
45. Carabali DM, Forero CR, Cadavid Y (2018) Energy diagnosis and structuring an energy saving proposal for the metal casting industry: an experience in Colombia. *Appl Therm Eng* 137:767–773. <https://doi.org/10.1016/j.applthermaleng.2018.04.012>
46. Dalquist S, Gutowski T (2004) Life Cycle Analysis of Conventional Manufacturing Techniques: Sand Casting, in: ASMEDC, International Mechanical Engineering Congress and Exposition, pp. 631–641
47. Huang R, Riddle ME, Graziano D, Das S, Nimbalkar S, Cresko J, Masanet E (2017) Environmental and economic implications of distributed additive manufacturing: the case of injection mold tooling. *J Ind Ecol* 21(1):130–143. <https://doi.org/10.1111/jiec.12641>
48. FOSECO (2020) *ECOLOTEC waterbased resole CO2 process*. [https://www.vesuvius.com/content/dam/vesuvius/corporate/Our-solutions/our-solutions-master-english/foundry/non-ferrous-foundry/binders/brochures/ECOLOTEC%20\(e\).pdf.downloadasset.pdf](https://www.vesuvius.com/content/dam/vesuvius/corporate/Our-solutions/our-solutions-master-english/foundry/non-ferrous-foundry/binders/brochures/ECOLOTEC%20(e).pdf.downloadasset.pdf). Accessed 03 May 2023
49. Mitterpach J, Hroncová E, Ladomerský J, Balco K (2017) Environmental analysis of waste foundry sand via life cycle assessment. *Environ Sci Pollut Res* 24:3153–3162. <https://doi.org/10.1007/s11356-016-8085-z>
50. Holtzer M, Daňko R, Daňko J (2018) Thermal utilization of the post reclamation dust from molding sand with furan resin in test unit. *Arch Foundry Eng* 18(4):15–18. <https://doi.org/10.24425/123625>
51. Pagone E, Saxena P, Papanikolaou M, Salonitis K, Jolly M (2021) Sustainability assessment of rapid sand mould making using multi-criteria decision-making mapping. In: Scholz SG, Howlett RJ, Setchi R (eds) *sustainable design and manufacturing 2020. Smart Innovation, Systems and Technologies*, vol 200. Springer, Singapore. [https://doi.org/10.1007/978-981-15-8131-1\\_31](https://doi.org/10.1007/978-981-15-8131-1_31)
52. Ngo TD, Kashani A, Imbalzano G, Nguyen KTQ, Hui D (2018) Additive manufacturing (3D printing): a review of materials, methods, applications and challenges. *Compos B Eng* 143:172–196. <https://doi.org/10.1016/j.compositesb.2018.02.012>
53. Singh S, Ramakrishna S, Gupta MK (2017) Towards zero waste manufacturing: a multidisciplinary review. *J Clean Prod* 168:1230–1243. <https://doi.org/10.1016/j.jclepro.2017.09.108>
54. Stock T, Seliger G (2016) Opportunities of sustainable manufacturing in industry 4.0. *Procedia CIRP* 40:536–541. <https://doi.org/10.1016/j.procir.2016.01.129>
55. Ciolfi F, Abbà A, Alias C, Sorlini S (2022) Reuse or disposal of waste foundry sand: an insight into environmental aspects. *Appl Sci* 12(13):6420. <https://doi.org/10.3390/app12136420>

56. Cheng YL, Tseng TW (2021) Study on driving waveform design process for multi-nozzle piezoelectric printhead in material-jetting 3D printing. *Rapid Prototyping Journal* 27(6):1172–1180. <https://doi.org/10.1108/RPJ-05-2019-0120>
57. Cheng YL, Li YT, Yang YT, Tang KT, Jhuang FA, Li KH, Lu CW (2022) Greyscale printing and characterization of the binder migration pattern during 3D sand mold printing. *Addit Manuf* 56:102929. <https://doi.org/10.1016/j.addma.2022.102929>
58. AFS (1982) AFS mold and core test handbook, American Foundrymen's Society, Inc., pp.3–1 ~ 17–10
59. Shan Zd, Guo Z, Du D, Liu F (2017) Coating process of multi-material composite sand mold 3D printing. *China Foundry* 14:498–505. <https://doi.org/10.1007/s41230-017-7078-y>
60. Chastain S, Chastain SD (2004) *Metal Casting: A Sand Casting Manual for the Small Foundry*, 2nd edn. Jacksonville, Florida, USA

**Publisher's Note** Springer Nature remains neutral with regard to jurisdictional claims in published maps and institutional affiliations.

Springer Nature or its licensor (e.g. a society or other partner) holds exclusive rights to this article under a publishing agreement with the author(s) or other rightsholder(s); author self-archiving of the accepted manuscript version of this article is solely governed by the terms of such publishing agreement and applicable law.